An epithelial-to-mesenchymal transition model recovers and predicts critical mutations underlying hepatic cancer stem cells emergence

Alexis Hernández-Magaña
Universidad Nacional Autónoma de México
Antonio Bensussen
Universidad de Colima
Juan Carlos Martínez-García (juancarlos.martinez@cinvestav.mx)
Cinvestav-IPN
Elena R. Álvarez-Buylla
Universidad Nacional Autónoma de México

Research Article

Keywords: Hepatocellular carcinoma, Cancer stem cells, Epithelial-to-Mesenchymal transition, Gene regulatory network, Medical Systems Biology

Posted Date: June 2nd, 2023

DOI: https://doi.org/10.21203/rs.3.rs-2877522/v1

Abstract

Background:

Cancer stem cells (CSCs) have the ability to form tumors, induce metastasis and resistance to chemotherapy. These cells are generated by the epithelium-mesenchymal transition, and its presence has been linked to a poor prognosis. In the case of hepatocellular carcinoma (HCC), it has been seen that the increase in stemness markers portends the death of the patient. Thus, it is essential to understand how CSCs are formed in order to improve treatments against HCC.

Results:

In the present work we carry out an exhaustive documentary investigation to create a gene regulatory network (GRN) in which a total number of 240 bibliographic references are integrated to model the epithelial-to-mesenchymal transition in hepatocytes (hEMT). From this network, we constructed a discrete Boolean model able to reproduce several apparently unconnected behaviors of the hEMT reported in the literature. We found that stem-like cells are formed by the action of hEMT only from proliferating hepatocytes in the WT model. Under normal conditions, stem-like cells are unstable and easily differentiate into other phenotypes. However, somatic mutations in tumor suppressors such as p53 or aberrant overexpression of oncogenes such as YAP1 stabilize proliferation conditions in hepatocytes and favor the appearance of CSCs. In addition, we found that these mutations have different effects on hEMT-mediated cell fates. Finally, our data suggest that this process is common to other epithelial cancers, but in HCC, inhibition of p53 is particularly important.

Conclusions:

In this work we found the mechanism by which somatic mutations generate the emergence of CSCs. These mechanisms may be used to understand the formation of CSCs in other epithelial cancers.

Background

Among the subtypes of hepatic cancer, hepatocellular carcinoma (HCC) is the most common of all (1, 2). According to data from 2020, 905,700 new cases were counted, and in the same year 830,200 patients died from this illness (3), throughout the world. The most common etiologic origin of HCC has been viral hepatitis, although, recently there have been more cases of HCC related to other etiological factors such as obesity, type 2 diabetes mellitus, and non-alcohol related fatty liver disease (NAFLD) (1, 2). This trend is particularly worrisome, since it is projected that liver cancer mortality may increase more than 55% by 2040 (3). The mortality of this cancer is associated to the ability of neoplastic cells to perform critical processes such as drug resistance, tumor recurrence, and metastasis. Recently, it has been observed that in several types of cancer, including HCC, there are small populations of cells with stem-like features, that are known as cancer stem cells (CSCs) (4, 5). Importantly, CSCs are implied in the cancer critical processes mentioned before (6). Moreover, it has been shown that CSCs can be originated from normal

stem/progenitor cells or through the dedifferentiation processes related to Epithelial-to-Mesenchymal transition (EMT) (7, 8).

Mechanically, EMT is a process by which epithelial cells lose polarity, cell-cell adhesion and acquire mesenchymal characteristics such as migratory capacity (9). These changes are associated with the downregulation of epithelial markers such as E-cadherin and miR200 microRNA family and upregulation of mesenchymal markers such as SNAI1 (Snail), SNAI2 (Slug), TWIST and ZEB (9, 10). EMT is involved in embryonic development, wound healing, and cancer-related aspects such as metastasis, therapy resistance (11–13) and aforementioned acquiring stem-like features (14–16). EMT in liver cancer context is regulated by a reciprocal inhibition circuit that promotes decreased expression of hepatocyte markers such as HNF1A, HNF4A, and increased expression of EMT inducers such as SNAI1 (Snail), SNAI2 (Slug) (17–20). It is noteworthy to mention that EMT inducers have also been related to the control of stem traits. Snail regulates the maintenance of resident liver stem cells and controls hepatocytes differentiation through a module that includes HNF4A, miR-200c, and miR-34a (21). Slug overexpression induces stemness and it controls NANOG and SOX2 expression in HCC (22, 23), and ZEB1 participates in a circuit with the miR-200 family that regulates stemness (24–26). Furthermore, OCT4 and NANOG promote EMT in HCC through STAT3-dependent activation of Snail (27).

Additionally, regulators of senescence, proliferation and inflammation such as p53, p21, β-catenin, YAP1, NF- κB and IL-6 are also associated with the control of EMT, as well as with stemness. In particular, p53 knockdown is able to potentiate TGF-β-induced EMT (28). Furthermore, p53 regulates the self-renewal and pluripotency of embryonic stem cells through the repression of genes such as OCT4, SOX2 and NANOG (29). On the other hand, p21 has been reported to form a complex with ZEB1 that inhibits EMT (30). Furthermore, p21 represses the expression of SOX2 by direct binding to its respective enhancer (31). Regarding β-catenin, it regulates the special properties of CSCs (32). In particular, β-catenin downregulates HNF4A expression and promotes EMT, and similarly, HNF4A inhibits Wnt/β-catenin pathway in HCC cells (18). Concerning to YAP1, it is also involved in the control of EMT and stemness by forming a circuit with HNF4A and Snail (33–35). In regard to inflammatory regulators, NF-κB induces EMT through upregulation of Snail, Slug, TWIST1, and ZEB1 (36). Finally, NF-κB (37) and IL-6 (15, 38) have been implicated as positive regulators of CSCs.

Despite having a vast amount of experimental information on EMT, it is still necessary to search for tools that allow integrating the data to unraveling the molecular complexity behind EMT. In this sense, previous dynamic models of gene regulatory networks (GRN) have been used to provide mechanistic understanding of cell differentiation and morphogenetic processes during normal and altered development from a system-biology perspective (39–42). This emerging field uses abstractions of the available information about gene regulation and signaling structures, to recover observed gene expression profiles characteristic of certain cell types. Such stable gene profiles are known as attractors and can be interpreted as phenotypes, depending on the process that is studied (40, 41, 43). Concerning to EMT, a previous gene regulatory network (GRN) discrete Boolean model, grounded on experimental evidence proposed a minimal generic transcriptional core gene regulatory module to understand EMT

(44). This Boolean model integrated regulators of proliferation, senescence, inflammation, epithelial markers and molecular signatures of mesenchymal phenotype and recovered three attractors corresponding to the observed expression profiles in epithelial, senescent epithelial, and stem-like mesenchymal cells (44). In this model, constitutive activation of NF-κB decreased the frequency of the epithelial phenotype and increased the frequency of the stem mesenchymal phenotype relative to the wild-type model (44), in agreement with the role of NF-κB as an inducer of EMT (36).

Here, we aimed to understand the specific regulatory processes by which CSCs are generated in HCC context. To this end, we integrated experimental evidence to propose a dynamic model of hepatocyte EMT gene regulatory network (hEMT). In methodological terms, we extended a generic EMT model (44) by incorporating regulatory modules described in normal hepatocytes and stem-cells. Our resulting discrete Boolean model recovers 8 attractors associated with the hepatocyte and mesenchymal phenotypes. Furthermore, analysis of the epigenetic landscape of our model shows that the loss of tumor suppressor genes such as p53, p16, p21 and RB, as well as the constitutive activation of TGF-β, NF-κB, β-catenin, and YAP1, increases the robustness of stem-like cells. These results provide a mechanism to understand how CSCs are originated in the specific context of HCC.

Results

Hepatocytes have genetic markers that influence EMT

In order to analyzing dynamical properties of EMT in HCC context, we first searched for genetic markers and molecular features that distinguish hepatocytes form other epithelial cells. We then incorporated such interactions to a previously published and validated model of EMT proposed by Méndez-López et al (44). In this model we added specific transcription factors (TFs) that have been described in hepatocyte differentiation such as HNF4A, HNF1A, FOXA2, and HNF6. These genetic markers belong to a cross-regulatory network that controls the development and adult function of the liver (45, 46). Particularly, it has been reported that HNF4 and HNF1A are negative regulators of Snail and Slug (17). Moreover, we incorporated TFs and interactions that are related to stemness and endodermal differentiation. In this sense, we added to the network OCT4, SOX2, NANOG and KLF4 because they are central regulators for the induction and maintenance of stem cells (47–49). It is noteworthy to mention that such TFs are involved in the emergence of a small stem-like cell population present in injured liver of mice (50).

Other genetic markers that have been incorporated to the network are GATA6, SOX9, β-catenin, YAP1 as well as miR-200a,b,c, and miR34a. Concerning each marker, GATA6 is essential for visceral endoderm differentiation and embryonic development of the liver (51, 52). SOX9 expression has been associated with proliferation and stem cell features in HCC (53). SOX9 is expressed in liver stem/progenitor cells but not in hepatocytes (54, 55). Wnt/β-catenin signaling pathway plays a pivotal role in liver development and regeneration (56). In particular, β-catenin regulates EMT in HCC cells through double-negative feedback with HNF4A (18). Regarding YAP1, it forms a circuit with SNAI1 and HNF4A (57), to regulate EMT (58), proliferation, and differentiation in HCC cells (59). The miR-200 family (miR-200a,b,c) and

miR34-a are involved in EMT (60), reprogramming (61), and differentiation (62). MiR-34a plays a role in EMT (63). SNAI1 and HNF4A regulate the expression of the miR-200 family and miR-34a. Grounded on experimental evidence of a total number of 240 papers (Additional File 1), we were able to postulate a regulatory network of 43 nodes that represents hEMT in the context of HCC (Fig. 1). We use all the information presented in this network to build a Boolean model of 43 logic rules, available in additional file 2 (Additional File 2).

hEMT is a source of phenotypic diversity

The network presented above, includes much of the complexity associated with hEMT. However, we seek to understand what is the effect of mutations observed in cancer cells on hEMT. For this reason, we decided to find the necessary and sufficient nodes to control the global dynamics of the GRN. To do this, we proceed to compact the network model using the algorithm proposed by Véliz-Cuba (64). Such procedure uses discrete math operations to simplify linear interactions, conserving all non-linear motives that contribute to the system dynamics, like positive and negative feedback loops (see Methods). Using this algorithm, we obtained a reduced network of 23 nodes (Fig. 2). In the same way, we validated our reduction by using the GINsim software (65). All Boolean logic rules of this reduced network are presented in additional file 3 (Additional File 3).

After reduction, we needed to know whether the simplified model of the hEMT network had preserved the essential dynamic information of the full model of GRN. To determine this, we characterized the dynamics of both Boolean models to find their attractors. In particular, for the simulation of the GRN full model we used 5,000,000 randomly selected configurations of the network as initial conditions. Then, we used the BoolNet R-package to find stable gene expression patterns known as attractors. In this case, the model converges to only 8 attractors that correspond to the following phenotypes: Senescent hepatocytes (SH), senescent mesenchymal cells (SM), quiescent hepatocytes (QH), quiescent mesenchymal cells (QM), proliferative hepatocytes (PH), proliferative mesenchymal cells (PM), proliferative stem-like hepatocytes (PSH), and proliferative stem-like mesenchymal cells (PMS) (Fig. 3a).

The mesenchymal phenotype was identified by the activation of SNAI1, SNAI2, TWIST1, ZEB1, FOXC2 (9, 66). The activation of HNF4A, HNF1A, HNF6 and FOXA2 correspond to the hepatocyte phenotype (45, 67). The senescent phenotype was identified by the activation of p53, p16, p21 and RB (68, 69). Proliferation was identified by E2F1 activation, cyclin D, and RB inactivation (70, 71). Quiescence was identified by RB and p21 activation, as well as by the absence of proliferation markers like E2F1, cyclin D, and the absence of senescence markers such as p53 and p16 (72). Furthermore, the stem-like phenotype was associated with the activation of OCT4, SOX2, and NANOG (49, 73).

On the other hand, the reduced model presented equivalent attractors (Fig. 3b), which indicates that set of nodes of this model is sufficient to describe the network dynamics. Finally, we compared the size of the basin of attraction for each phenotype. This was done for both the full model (Fig. 3c) and the reduced model (Fig. 3d). We observed that such results are qualitatively congruent with each other. Remarkably,

PMS and PSH presents stem-like features given by the activity of NANOG, OCT4 and SOX2 (Fig. 3a and 3b), which implies that such phenotypes have self-renewal properties. Moreover, the size of the basin of attraction of PMS and PSH indicates that such phenotypes are less frequent than others (Fig. 3c and 3d), which is congruent with the low prevalence of stem-cells in nature (74). Collectively these results indicate that the reduced model is capable of capturing the biological richness of the extended model, and it will therefore be used to assess the effect of mutations on hEMT.

Phenotypes produced by hEMT GRN are robust and physiologically feasible

The results presented above show that hEMT GRN reproduces a set of well-defined hepatic phenotypes. In physiological context, phenotypes persist even in presence of slight molecular changes such as alterations produced by viral infections, thermal changes, osmotic pressure adaptations among other stressor stimuli (75). For this reason, we wanted to determine whether these phenotypes produced by hEMT model are able to persist in presence of physiological changes. To do this, we tested the robustness of the GRN in presence of fluctuations by starting Boolean simulations with all states of the network as an initial conditions, and then applying stochastic noise to the logical rules of the nodes in order to determine whether the state belongs to the same basin of attraction or whether it transits to a different basin (76). As a result of this procedure, we determine the probabilities that an hEMT-produced phenotype remains fixed or to change towards other phenotypes randomly (Fig. 4a). Numerically, we found the probabilities that the phenotypes are maintained in the face of fluctuations are greater than 0.9, which indicates that such phenotypes are robust, and therefore physiologically feasible (Fig. 4b).

Current biological observations of hEMT are mechanistically explained by the GRN

After determined the feasibility of the minimal hEMT model under stochastic physiological conditions, we wanted to test its effectiveness as a predictive tool. To this end, we simulate a series of loss-or-gain-of-function mutations on a particular set of genes like SNAI1, SNAI2, HNF1A and HNF4A as well as oncogenes as YAP1 and β-catenin. In the same way, we studied the effects of targeting tumor suppressors such as p53, p21, p16 and RB (Fig. 5a and Additional File 4). To simulate the gain of function, we set the value of the target node as one. Similarly, to simulate the loss of function, we set the value of the target node to zero for all time-steps of simulation. Then, for each mutated network we calculated its attractors with their respective basin sizes. Finally, we analyze the impact (ΔS_i) that each mutation has on the WT attractor landscape by subtracting the value of each wild-type basin (S_{WT}) from the value of the mutated basin (S_i), that is: $\Delta S_i = S_i - S_{WT}$ (Fig. 5b).

As a result of these assays, the model proved to be highly predictive, since it was able to qualitatively reproduce several experimental observations such as, either the inhibition of HNF4A and HNF1A or the overexpression of SNAI1 and SNAI2 are able to increase the mesenchymal phenotype (Fig. 5b and

Table 1). The opposite occurs when HNF4A and HNF1A are overexpressed, increasing the hepatocyte phenotype (Fig. 4d and Table 1). In the same direction, inhibition of p53, p16 and p21 reduces senescent phenotypes (Fig. 5b and Table 1), while the opposite occurs when p53 and p16 are overexpressed (Fig. 5b and Table 1). Regarding proliferation, the model showed that it can be triggered when p21, p16, p53 and RB are inhibited or alternatively when YAP1 and β-catenin are overexpressed (Fig. 5b and Table 1). Finally, the model also showed that the constitutive activation of YAP1 increases the stem-like phenotype (Fig. 5b and Table 1). Collectively, these results validate our qualitative model as a predictive tool.

Table 1
Validation of the hEMT model

Mutation*	Prediction**	Experimental outcomes	References
KO HNF4A	This condition increases mesenchymal cells.	HNF4A silencing increased migratory capacity and the expression of mesenchymal markers.	(77)
KO HNF1A	This condition increases mesenchymal cells.	This increases cell's migratory capacity and the expression of mesenchymal markers.	(77)
KO SNAI1	This condition reduces mesenchymal cells.	SNAI1 silencing decreased migratory capacity and the expression of mesenchymal markers.	(78,79)
KO p53	This condition reduces senescence.	p53 deletion reduces senescence.	(68,80,81)
KO p16	This condition reduces senescence.	p16 deletion reduces senescence.	(82)
KO p21	It reduces senescence and increases proliferation.	p21 deletion reduces senescence and increases proliferation.	(83,84)
KO RB	This condition increases proliferation.	RB deletion increases proliferation.	(83,85,86)
OE HNF4A	This condition reduces mesenchymal cells.	HNF4A overexpression increases epithelial morphology and reduces motility as well as invasive capacity.	(77,78)
OE SNAI1	This condition increases mesenchymal cells.	SNAI1 overexpression increase mesenchymal phenotype.	(78,79,87)
OE SNAI2	This condition increases mesenchymal cells.	SNAI2 overexpression increase mesenchymal phenotype.	(17,19)
OE β-catenin	This condition increases proliferation.	β-catenin activation promotes proliferation.	(88,89).
OE YAP1	This condition increases stem-like phenotype.	YAP1 activation increase stem-like phenotype.	(35)
OE p53	This condition increases senescence.	p53 activation promotes senescence.	(90)
OE p16	This condition increases senescence.	p16 overexpression promotes senescence.	(82)

*KO means 'knockout' and OE is 'overexpression'. **All predictions were taken from Fig. 5b.

Hepatocytes and epithelial cells can be transformed into CSCs in a similar way

The analysis of mutations on hEMT GRN showed that there are genes capable of biasing the process towards proliferative phenotypes, including the PMS phenotype (Fig. 6a and 6b). Consequently, we decided to investigate the effect on the robustness of attractors produced by the loss of function of the tumor suppressors p53, p21, p21 and RB, as well as the overexpression of YAP1 and β-catenin oncogenes. Regarding the phenotype robustness, we observed that all simulated mutations enhance proliferative phenotypes, including PMS (Fig. 6c), while senescent phenotypes were only affected by inhibition of p53 (Fig. 6d). Interestingly, mutations on tumor suppressors as well as oncogenes favor the appearance of proliferative stem-like phenotypes (Fig. 6d). We hypothesize that this augment in stem-like phenotypes corresponds to the appearance of CSCs, represented by PMS and PSH phenotypes.

It is not clear whether this property is exclusive to hepatocytes or not. To explore this issue, we compared the impact of each mutation (ΔS_i) on the WT attractor landscape of HCC against Méndez-López et al (44) observations in various types of cancers (Fig. 6e). Qualitatively, the behavior of hepatocytes was similar to other epithelial cells. However, it is notable that hepatocytes were less sensitive to SNAI2 mutations. In fact, SNAI2 did not induce serious alterations in senescent phenotypes compared to that seen in other epithelial cells (Fig. 6e). Furthermore, we noted that KO p53 strongly reduced senescent phenotypes in liver compared to other epithelial cells (Fig. 6e). Collectively, these results may suggest that there might be a common mechanism in the appearance of CSCs for epithelial cells, but it could be affected by the genetic characteristics of each cell type.

Mutations on oncogenes and tumor suppressors generate CSCs

Next, we wanted to determine what the most likely phenotypic transitions are. To investigate this point we use the mean first passage time (MFPT), which is a metric to determine how difficult it is for a GRN to take the first step in a differentiation trajectory towards another phenotype. In general, the MFPT is used to calculate the net transition rate, which determines how easy it is to move from one state to another (see Methods). As a result of this procedure, we observed no transitions from senescent phenotypes to proliferative or quiescent phenotypes in WT model (Fig. 7a), which confirms the stability of the senescent phenotypes suggested by the size of the attraction basins. We also noted that transitions towards proliferative and stem-like phenotypes are relatively low (Fig. 7a). In the WT model, the attractors associated with the quiescent and senescent phenotypes are the most stable.

Finally, we examined how mutations could affect the probabilities of phenotypic transitions. To do this, we simulated the most common mutations presented in HCC and other cancers, which are: loss-of-function mutations of RB, p21, p16, p53, as well as constitutive activation of β-catenin, YAP1, NF-kB, and TGF-β. As a result of these simulations, we found that aberrant activation of β-catenin, YAP1, NF-kB, and

TGF-β increased the index of net transition of proliferative hepatocytes to proliferative mesenchymal cells (Fig. 7b), in concordance with previous experimental observations (10, 33, 36). On the other hand, the loss-of-function of tumor suppressor genes like p16, p21 and p53 increased this transition (Fig. 7b), in agreement with similar *in vitro* assays (28, 30, 91). All simulated alterations promoted transition from hepatocytes with stem-like features to mesenchyme with stem-like phenotype. However, only p53 loss-of-function mutations as well as constitutive activation of NF-κB and TGF-β favored the transition of proliferative hepatocytes to proliferative mesenchyme with stem-like phenotype (Fig. 7b). Thus, these mutations are essential to increase the prevalence of CSCs.

Discussion

Hepatocellular carcinoma (HCC) is a type of cancer with a high mortality rate, and increasing the expression of CSCs markers is associated with a poor prognosis of such neoplasm (92). This suggests that CSCs could be the origin of mortality associated with HCC. Recent evidence has shown that CSCs are a heterogeneous group of cells, since there may be several phenotypes with different levels of expression of epithelial and mesenchymal markers (93). In this regard, it has been reported that proliferative CSCs displaying an abundance of mesenchymal markers has the ability to initiate tumors, resist chemotherapy, and they are able to trigger metastasis (93). In contrast, proliferative CSCs with a predominance of epithelial markers lose their ability to initiate metastasis (93). It is known that CSCs can be originated from EMT, although the detailed process remains to be elucidated.

Then, it is essential to understand the exact emergence mechanism of CSCs in the liver. For this reason, in the present work we built a dynamic regulatory network model to explain the epithelial-to-mesenchymal transition in hepatocytes (hEMT). Our Boolean model was supported by 240 experimental reports (Additional File 1), and despite the fact that our model is qualitative and synchronous in its computational implementation, it was able to explain several experimental observations of hEMT (Fig. 5b and Table 1). In this sense, our model predicted the existence of eight attractors (Fig. 3a and 3b), which correspond to the following cell phenotypes: senescent hepatocytes (SH), proliferative hepatocytes (PH), quiescent hepatocytes (QH), proliferative stem-like hepatocytes (PSH), senescent mesenchymal cells (SM), proliferative mesenchymal cells (PM), quiescent mesenchymal cells (QM) and proliferative stem-like mesenchymal cells (PMS). Remarkably, after a careful analysis of gene expression patterns of attractors, we noted that mesenchymal CSCs and epithelial CSCs were reproduced by our model after mutate WT network. In such case, PMS may be equivalent to mesenchymal CSCs and PSH may correspond to epithelial CSCs since both cells are NANOG + OCT4 + SOX2 + with mesenchymal and epithelial markers, respectively (Fig. 3a and 3b). Thus, these results demonstrate that our qualitative model is a satisfactory predictive tool, capable to track the emergence of CSCs.

Now, the question to answer is how CSCs are formed in HCC context. In this direction, our model showed that stem-like cells are formed naturally as a result of hEMT dynamics. However, these phenotypes have low robustness (Fig. 3c and 3d), which means that such cells tend to easily differentiate into other phenotypes (Fig. 7a). In consequence, this prevents the spontaneous formation of tumors. Nevertheless,

somatic mutations such as inhibition of tumor suppressors like p53, as well as aberrant expression of oncogenes like YAP1, can drastically increase the prevalence of CSCs (Fig. 5). In fact, our simulations show that mutations in tumor suppressors can generate distinct differentiation pathways. For example, in the case of RB inhibition, the transition of PSH towards PMS cells is favored, while the differentiation of PH towards PMS is hindered (Fig. 7b). Mechanistically, the loss of function of p16, p21 or p53 simultaneously decreases the stability of senescence and stabilizes proliferative phenotypes, increasing CSCs (Fig. 7b).

Finally, it is necessary to determine whether this mechanism to generate CSCs is universal for all types of epithelial cancers, or whether it is a specific mechanism for HCC. Regarding this point, our results suggest that such mechanism is common for all epithelial cancers, however, hepatocytes present its own particularities (Fig. 6e). For instance, our results shows that suppression of p53 is especially important to form CSCs in HCC context (Fig. 6e), which may explain why p53 deletions drastically increase HCC mortality (94). In general, our model shows that somatic mutations affect the stability of the attractors and the transitions between them, although the intracellular network still maintains its multistability, which implies that mutated cells retain their plasticity. This might explain, the phenotypic heterogeneity of tumor cells, since multiple phenotypes emerge from the same mutated network, although their robustness and transition probabilities may vary from the WT model.

We hypothesize that tracking changes in probability and robustness against perturbations of phenotypes might be a useful approach for either proposing or testing novel therapeutic strategies against HCC. There is still much more to investigate about the origin of CSCs in other cell types, but now is clear that the phenotypic heterogeneity presented by these cells is due to the plasticity of an underlying multistable GRN.

Conclusions

Our study strongly supports the conclusion that stem-like cells in liver are generated from proliferating hepatocytes and in a natural context they are not stable. Somatic mutations in tumor suppressors such as p53, RB, p21 and p16, as well as aberrant expression of oncogenes such as YAP1, increase proliferation conditions, which consequently favors the formation of CSCs. Finally, the CSCs generation process may be common to all type of epithelial cancers, but in hepatocytes inhibition of p53 increases CSCs stability.

Methods

Construction of the network

We expanded the qualitative discrete Boolean model of EMT proposed by Méndez-López et al (44) by adding transcription factors as well as other proteins that are specific markers of liver cells. We also consulted 240 experimental references to obtain details about regulatory connections between markers.

Furthermore, we manually select relevant and documented interactions to construct our gene regulatory network of hepatocytes (Fig. 1).

Derivation of Boolean model

Each molecular component represented as network nodes or Boolean variables may have two categorical states: "activated" or "inactivated". Numerically, such states can be represented by the elements of the set {0,1} as follows: 0 for "inactivated" and 1 for "activated". The transition of state for all network nodes is a logical function f that depends on the previous state of other nodes, that is:

$$x_i(t+\tau) = f_i(x_1(t), x_2(t), \ldots x_k(t))$$

,

Where $x_i(t+\tau)$ is the current state of the node i at time $t+\tau$, f_i is the logic function that controls state transition depending on the previous state of nodes $x_1(t), x_2(t), \ldots x_k(t)$. Importantly, each logic function was constructed using logic operators {AND, NOT, OR}, depending on the context of biological interactions of each molecular node of the network (43, 95).

Reduction of the network

The complexity of the network was reduced without losing its essential biological information using the following algorithm (64): For each node removed (y_j) with an associated function f_{y_j} such that f_{y_j} does not depend on y_j: 1) If z, with an associated function f_z, was a vertex governed by y_j, then the function $f_z\left(y_1, \ldots, y_j, \ldots, y_k\right)$ was replaced by $f_z\left(y_1, \ldots, f_{y_j}, \ldots, y_k\right)$. 2) Then, f_z was simplified using Boolean algebra to remove non-functional variables. 3) If the node x regulates the node y_j and y_j regulates the node z, that is: $x \to y_j$ and $y_j \to z$, we placed: $x \to z$. Finally, we verify the reduction of the model using the GINsim software (65).

Computational implementation

We use the R-package BoolNet (96) to calculate the fixed point attractors for both models, the GRN reduced one and the GRN original one. In both cases we use the synchronous and asynchronous update scheme. Using this R-package, we also calculated the size of the basins of attraction for each fixed point, that is the set of network configurations that converges on a specific attractor.

Robustness of the Boolean model

To test the robustness of the network against stochastic perturbations, we first solve the Boolean model of the network. After that, we pick each attractor of the model, and we set it as initial configuration of the network. At each time step of the simulation, stochastic noise was applied to the network given by the following equation:

$$x_i\left(t+\tau\right)=\begin{cases} f_i\left(t\right), & if P=1-\eta \\ 1-f_i\left(t\right), & if P=\eta \end{cases}$$

The probability that each logical rule obeyed its normal behavior, or changed, was calculated. In all cases, the probability of error for the logical rule was set as $\eta = 0.01$. At the end of each simulation, it was determined if the attractor had remained unchanged, or if it had transited to another attractor, or associated basin of attraction. Each event change was counted, and this procedure was repeated for 1000 times. Finally, the number of times each basin of attraction was reached was divided by the total number of initial configurations of each basin. The diagonal of the Markov matrix that we obtain indicates the probability of staying in the same basin of attraction (76). The probability close to 1 indicates that the model is robust. This procedure was implemented with the R-script previously published by (44).

Stability of the network

We tested the relative stability of each fixed point by calculating the mean first passage time (MFPT), that is the number of average steps required to transit from an attractor i to an attractor j for the first time. The value of the MFPT is proportional to the barrier or difficulty to transit between two given attractors, which means this metrics quantifies the barrier to transition among phenotypes. We calculated the MFPT from the transition probability matrix following the procedure and R-scripts described by (44).

Based on MFPT, the network transition index between two attractors (d_{ij}) was calculated as follows:

$$d_{ij}=\frac{1}{MFPT_{i,j}}-\frac{1}{MFPT_{j,i}}$$

Where d_{ij} > 0 implies that attractor i is more stable than attractor j.

Validation

To validate the model, loss and gain-of-function mutations were simulated and verifying that the behavior of the model corresponded to the experimental qualitative observations. All gain-of-function mutations were implemented by setting to one the value of each mutated node. Similarly, for all loss-of-function mutations the value of mutated nodes was fixed at zero.

Abbreviations

HCC
Hepatocellular carcinoma.
NAFLD
Non-alcohol related fatty liver disease.
CSCs
Cancer stem cells.
EMT

Epithelial-to-Mesenchymal transition.
hEMT
hepatocyte EMT gene regulatory network.
TFs
Transcription factors.
SH
Senescent hepatocytes.
SM
Senescent mesenchymal cells.
QH
Quiescent hepatocytes.
QM
Quiescent mesenchymal cells.
PH
Proliferative hepatocytes.
PM
Proliferative mesenchymal cells.
PSH
Proliferative stem-like hepatocytes.
PMS
Proliferative stem-like mesenchymal cells.

Declarations

Ethics approval and consent to participate

Not applicable.

Consent for publication

All authors agree to publish the manuscript.

Availability of data and materials

The experimental data that sustains the GRN and their references are available in additional text file 1 (see Additional File 1). The complete unreduced GRN model is available in additional text file 2 (see Additional File 2). The reduction data, along with the reduced GRN model, are available at additional text file 3 (see Additional File 3). The network attractors with their corresponding basin of attraction obtained by the loss and gain-of-function simulations are available in additional text file 4 (see Additional File 4).

Competing interests

The authors declare that they have no conflict of interest.

Fundings

Elena R. Álvarez-Buylla and Juan Carlos Martínez-García acknowledge the support from UNAM-DGAPA PAPIIT IN211721 “Patrones genéricos y sistémicos de la diferenciación y la proliferación en los nichos de células troncales: Raíz de Arabidopsis thaliana como sistema de estudio teórico-experimental” and CONACYT-FORDECYT-PRONACES 194186/2020 “Biología matemática y computacional de sistemas médicos: modulación preventive de la emergencia y progresión de enfermedades crónico-degenerativas.”, respectively.

Authors’ contributions

All authors participated in draft redaction, conceptualization and discussion of data. AHM constructed the model, searched for experimental data, performed simulations and interpreted the data. AB draw graphics, prepared and interpreted the data. ERAB and JCMG conceptualized, supervised and provided resources.

Acknowledgement

AHM and AB thank to CONACYT for their doctoral and postdoctoral fellowships respectively.

References

1. Marengo A, Rosso C, Bugianesi E. Liver Cancer: Connections with Obesity, Fatty Liver, and Cirrhosis. Annu Rev Med. 2016;67:103–17.
2. Konyn P, Ahmed A, Kim D, Konyn P, Ahmed A. Current epidemiology in hepatocellular carcinoma. Expert Rev Gastroenterol Hepatol. 2021;15(11):1295–308.
3. Rumgay H, Arnold M, Ferlay J, Lesi O, Cabasag CJ, Vignat J et al. Global burden of primary liver cancer in 2020 and predictions to 2040. J Hepatol [Internet]. 2022 Dec 1;77(6):1598–606. Available from: https://www.journal-of-hepatology.eu/article/S0168-8278(22)03022-7/abstract
4. Ma S, Chan KW, Hu L, Lee TKW, Wo JYH, Ng IOL, et al. Identification and Characterization of Tumorigenic Liver Cancer Stem/Progenitor Cells. Gastroenterology. 2007;132(7):2542–56.
5. Yagci T, Cetin M, Ercin PB. Cancer Stem Cells in Hepatocellular Carcinoma. J Gastrointest Cancer. 2017;48(3):241–5.
6. Wu Y, Zhang J, Zhang X, Zhou H, Liu G, Li Q. Cancer Stem Cells: A Potential Breakthrough in HCC-Targeted Therapy. Front Pharmacol. 2020;11(March):1–13.
7. Wang K, Sun D. Cancer stem cells of hepatocellular carcinoma. 2018;9(33):23306–14.
8. Nio K, Yamashita T, Kaneko S. The evolving concept of liver cancer stem cells. Mol Cancer. 2017;16(1):1–12.
9. Kalluri R, Weinberg RA. Review series The basics of epithelial-mesenchymal transition. 2009;119(6).

10. Giannelli G, Koudelkova P, Dituri F, Mikulits W. Role of epithelial to mesenchymal transition in hepatocellular carcinoma. J Hepatol. 2016;65(4):798–808.
11. Ribatti D, Tamma R, Annese T. Translational Oncology Epithelial-Mesenchymal Transition in Cancer: A Historical Overview. Transl Oncol. 2020;13(6):100773.
12. Chen T, You Y, Jiang H, Wang ZZ. Epithelial–mesenchymal transition (EMT): A biological process in the development, stem cell differentiation, and tumorigenesis. J Cell Physiol. 2017;232(12):3261–72.
13. Thiery JP. Epithelial–mesenchymal transitions in tumour progression. Nat Rev Cancer. 2002;2(6):442–54.
14. Mani SA, Guo W, Liao MJ, Eaton EN, Ayyanan A, Zhou AY, et al. The Epithelial-Mesenchymal Transition Generates Cells with Properties of Stem Cells. Cell. 2008;133(4):704–15.
15. Xie G, Yao Q, Liu Y, Du S, Liu A, Guo Z, et al. IL-6-induced epithelial-mesenchymal transition promotes the generation of breast cancer stem-like cells analogous to mammosphere cultures. Int J Oncol. 2012;40(4):1171–9.
16. Jayachandran A, Dhungel B, Steel JC. Epithelial-to-mesenchymal plasticity of cancer stem cells: therapeutic targets in hepatocellular carcinoma. J Hematol Oncol. 2016;1–12.
17. Santangelo L, Marchetti A, Cicchini C, Conigliaro A, Conti B, Mancone C, et al. The stable repression of mesenchymal program is required for hepatocyte identity: A novel role for hepatocyte nuclear factor 4α. Hepatology. 2011;53(6):2063–74.
18. Yang M, Li SN, Anjum KM, Gui LX, Zhu SS, Liu J, et al. A double-negative feedback loop between Wnt-β-catenin signaling and HNF4α regulates epithelial-mesenchymal transition in hepatocellular carcinoma. J Cell Sci. 2013;126(24):5692–703.
19. Pelletier L, Rebouissou S, Vignjevic D, Bioulac-sage P. Zucman-rossi J. HNF1 a inhibition triggers epithelial-mesenchymal transition in human liver cancer cell lines. 2011;3:1–11.
20. Cicchini C, Amicone L, Alonzi T, Marchetti A, Mancone C, Tripodi M. Molecular mechanisms controlling the phenotype and the EMT/MET dynamics of hepatocyte. Liver Int. 2015;35(2):302–10.
21. Garibaldi F, Cicchini C, Conigliaro A, Santangelo L, Cozzolino AM, Grassi G, et al. An epistatic mini-circuitry between the transcription factors Snail and HNF4α controls liver stem cell and hepatocyte features exhorting opposite regulation on stemness-inhibiting microRNAs. Cell Death Differ. 2012;19(6):937–46.
22. Sun YU, Song GUOD, Sun N, Chen JQIU, Yang SSHI. Slug overexpression induces stemness and promotes hepatocellular carcinoma cell invasion and metastasis. 2014;1936–40.
23. Zhao X, Sun B, Sun D, Liu T, Che N. Slug promotes hepatocellular cancer cell progression by increasing sox2 and nanog expression. 2015;149–56.
24. Wellner U, Schubert J, Burk UC, Schmalhofer O, Zhu F, Sonntag A et al. The EMT-activator ZEB1 promotes tumorigenicity by repressing stemness-inhibiting microRNAs. Nat Cell Biol. 2009;11(12).
25. Bracken CP, Gregory PA, Kolesnikoff N, Bert AG, Wang J, Shannon MF, et al. A double-negative feedback loop between ZEB1-SIP1 and the microRNA-200 family regulates epithelial-mesenchymal

transition. Cancer Res. 2008;68(19):7846–54.
26. Tsai S-C, Lin C-C, Shih T-C, Tseng R-J, Yu M-C, Lin Y-J, et al. The miR-200b-ZEB1 circuit regulates diverse stemness of human hepatocellular carcinoma. Mol Carcinog. 2017 Sep;56(9):2035–47.
27. Yin X, Zhang B, Zheng S, Gao D, Qiu S, Wu W et al. Coexpression of gene Oct4 and Nanog initiates stem cell characteristics in hepatocellular carcinoma and promotes epithelial-mesenchymal transition through activation of Stat3 / Snail Signal. 2015;1–13.
28. Wang Z, Jiang Y, Guan D, Li J, Yin H, Pan Y et al. Critical Roles of p53 in Epithelial-Mesenchymal Transition and Metastasis of Hepatocellular Carcinoma Cells. 2013;8(9).
29. Li M, He Y, Dubois W, Wu X, Shi J, Huang J. Article Distinct Regulatory Mechanisms and Functions for p53-Activated and p53-Repressed DNA Damage Response Genes in Embryonic Stem Cells. Mol Cell. 2012;46(1):30–42.
30. Li XL, Hara T, Choi Y, Subramanian M, Francis P, Bilke S, et al. A p21-ZEB1 Complex Inhibits Epithelial-Mesenchymal Transition through the MicroRNA 183-96-182 Cluster. Mol Cell Biol. 2014;34(3):533–50.
31. Yamamizu K, Schlessinger D, Ko MSH. SOX9 accelerates ESC differentiation to three germ layer lineages by repressing SOX2 expression through P21 (WAF1/CIP1). Dev. 2014;141(22):4254–66.
32. Leung RWH, Lee TKW. Wnt/β-Catenin Signaling as a Driver of Stemness and Metabolic Reprogramming in Hepatocellular Carcinoma. Cancers (Basel). 2022 Nov;14(21).
33. Noce V, Battistelli C, Cozzolino AM, Consalvi V, Cicchini C, Strippoli R et al. YAP integrates the regulatory Snail/HNF4α circuitry controlling epithelial/hepatocyte differentiation. Cell Death Dis. 2019;10(10).
34. Cai WY, Lin LY, Hao H, Zhang SM, Ma F, Hong XX, et al. Yes-associated protein/TEA domain family member and hepatocyte nuclear factor 4-alpha (HNF4α) repress reciprocally to regulate hepatocarcinogenesis in rats and mice. Hepatology. 2017;65(4):1206–21.
35. Zhu C, Li L, Zhao B. The regulation and function of YAP transcription. 2015;47(December 2014):16–28.
36. Min C, Eddy SF, Sherr DH, Sonenshein GE. NF- k B and Epithelial to Mesenchymal. Transition of Cancer. 2008;744:733–44.
37. Czauderna C, Castven D, Mahn FL, Marquardt JU. Context-Dependent Role of NF-κB Signaling in Primary Liver Cancer—from Tumor Development to Therapeutic Implications. Cancers (Basel). 2019;11(8):1053.
38. Xu J, Lin H, Wu G, Zhu M, Li M. IL-6 / STAT3 Is a Promising Therapeutic Target for Hepatocellular Carcinoma. 2021;11(December):1–14.
39. Ortiz-gutiérrez E, García-cruz K, Azpeitia E, Castillo A. A Dynamic Gene Regulatory Network Model That Recovers the Cyclic Behavior of Arabidopsis thaliana Cell Cycle. 2015;(Cc):1–28.
40. Weinstein N, Mendoza L, Álvarez-buylla ER. Comput Model Endothelial Mesenchymal Transition. 2020;11(March).

41. Martinez-Sanchez ME, Mendoza L, Villarreal C, Alvarez-Buylla ER. A Minimal Regulatory Network of Extrinsic and Intrinsic Factors Recovers Observed Patterns of CD4 + T Cell Differentiation and Plasticity. PLOS Comput Biol [Internet]. 2015 Jun 19;11(6):e1004324. Available from: https://journals.plos.org/ploscompbiol/article?id=10.1371/journal.pcbi.1004324.
42. García-Gómez ML, Azpeitia E, Álvarez-Buylla ER. A dynamic genetic-hormonal regulatory network model explains multiple cellular behaviors of the root apical meristem of Arabidopsis thaliana. PLoS Comput Biol. 2017 Apr;13(4):e1005488.
43. Alvarez-buylla ER. Dynamic network-based epistasis analysis. Boolean examples. 2011;2(December):1–12.
44. Méndez-López LF, Davila-Velderrain J, Domínguez-Hüttinger E, Enríquez-Olguín C, Martínez-García JC, Alvarez-Buylla ER. Gene regulatory network underlying the immortalization of epithelial cells. BMC Syst Biol. 2017;11(1):24.
45. Lau HH, Hui N, Ng J, Sai L, Loo W, Jasmen JB, et al. The molecular functions of hepatocyte nuclear factors – In and beyond the liver. J Hepatol. 2018;68(5):1033–48.
46. Kyrmizi I, Hatzis P, Katrakili N, Tronche F, Gonzalez FJ, Talianidis I. Plasticity and expanding complexity of the hepatic transcription factor network during liver development. Genes Dev. 2006;20(16):2293–305.
47. Loh Y, Wu Q, Chew J, Vega VB, Zhang W, Chen X et al. The Oct4 and Nanog transcription network regulates pluripotency in mouse embryonic stem cells. 2006;38(4):431–40.
48. Jiang J, Chan YS, Loh YH, Cai J, Tong GQ, Lim CA, et al. A core Klf circuitry regulates self-renewal of embryonic stem cells. Nat Cell Biol. 2008;10(3):353–60.
49. Chen X, Xu H, Yuan P, Fang F, Huss M, Vega VB et al. Integration of external signaling pathways with the core transcriptional network in embryonic stem cells. Cell 2008 Jun;133(6):1106–17.
50. Cao W, Chen K, Bolkestein M, Yin Y, Verstegen MMA, Bijvelds MJC, et al. Dynamics of Proliferative and Quiescent Stem Cells in Liver Homeostasis and Injury. Gastroenterology. 2017;153(4):1133–47.
51. Zhao R, Watt AJ, Li J, Luebke-wheeler J, Morrisey EE, Duncan SA. GATA6 Is Essential for Embryonic Development of the Liver but Dispensable for. Early Heart Formation. 2005;25(7):2622–31.
52. Morrisey EE, Tang Z, Sigrist K, Lu MM, Jiang F, Ip HS et al. GATA6 regulates HNF4 and is required for differentiation of visceral endoderm in the mouse embryo. 1998;3579–90.
53. Richtig G, Aigelsreiter A, Schwarzenbacher D, Ress AL, Adiprasito JB, Stiegelbauer V, et al. SOX9 is a proliferation and stem cell factor in hepatocellular carcinoma and possess widespread prognostic significance in different cancer types. PLoS ONE. 2017;12(11):1–15.
54. Tarlow BD, Pelz C, Milton J, Grompe M, Tarlow BD, Pelz C, et al. Bipotential Adult Liver Progenitors Are Derived from Chronically Injured Mature Hepatocytes Article Bipotential Adult Liver Progenitors Are Derived from Chronically Injured Mature Hepatocytes. Stem Cell. 2014;15(5):605–18.
55. Paganelli M, Nyabi O, Sid B, Evraerts J, El Malmi I, Heremans Y, et al. Downregulation of Sox9 expression associates with hepatogenic differentiation of human liver mesenchymal stem/progenitor cells. Stem Cells Dev. 2014 Jun;23(12):1377–91.

56. Perugorria MJ, Olaizola P, Labiano I, Esparza-Baquer A, Marzioni M, Marin JJG, et al. Wnt–β-catenin signalling in liver development, health and disease. Nat Rev Gastroenterol Hepatol. 2019;16(2):121–36.
57. Lee DH, Park JO, Kim TS, Kim SK, Kim TH, Kim MC, et al. LATS-YAP/TAZ controls lineage specification by regulating TGFβ signaling and Hnf4α expression during liver development. Nat Commun. 2016;7(May):1–14.
58. Oh SH, Swiderska-Syn M, Jewell ML, Premont RT, Diehl AM. Liver regeneration requires Yap1-TGFβ-dependent epithelial-mesenchymal transition in hepatocytes. J Hepatol. 2018;69(2):359–67.
59. Fitamant J, Kottakis F, Benhamouche S, Tian HS, Chuvin N, Parachoniak CA, et al. YAP Inhibition Restores Hepatocyte Differentiation in Advanced HCC, Leading to Tumor Regression. Cell Rep. 2015;10(10):1692–707.
60. Mongroo PS, Rustgi AK. The role of the miR-200 family in epithelial-mesenchymal transition. Cancer Biol Ther. 2010;10(3):219–22.
61. Wang G, Guo X, Hong W, Liu Q, Wei T, Lu C, et al. Critical regulation of miR-200/ZEB2 pathway in Oct4/Sox2-induced mesenchymal-to-epithelial transition and induced pluripotent stem cell generation. Proc Natl Acad Sci U S A. 2013;110(8):2858–63.
62. Kim Y, Kim N, Park SW, Kim H, Park HJ, Han YM. Lineage-specific expression of miR-200 family in human embryonic stem cells during in vitro differentiation. Int J Stem Cells. 2017;10(1):28–37.
63. Imani S, Wei C, Cheng J, Khan A. MicroRNA-34a targets epithelial to mesenchymal transition-inducing transcription factors (EMT-TFs) and inhibits breast cancer cell migration and invasion. 2017;8(13):21362–79.
64. Veliz-Cuba A. Reduction of Boolean network models. J Theor Biol. 2011;289(1):167–72.
65. Chaouiya C, Naldi A, Thieffry D. Logical modelling of gene regulatory networks with GINsim. Methods Mol Biol. 2012;804:463–79.
66. Sistigu A, Di Modugno F, Manic G, Nisticò P. Deciphering the loop of epithelial-mesenchymal transition, inflammatory cytokines and cancer immunoediting. Cytokine Growth Factor Rev. 2017;36:67–77.
67. Odom DT, Zizlsperger H, Gordon DB, Bell GW, Rinaldi NJ, Murray HL et al. Control of Pancreas and Liver Gene Expression by HNF Transcription Factors. Science (80-). 2004;303(5662):1378–81.
68. Huda N, Liu G, Hong H, Yan S, Khambu B, Yin X. Hepatic senescence, the good and the bad. 2019;25(34):5069–81.
69. Ozturk M, Arslan-ergul A, Bagislar S, Senturk S, Yuzugullu H. Senescence and immortality in hepatocellular carcinoma. Cancer Lett. 2009;286(1):103–13.
70. Mullany LK, White P, Hanse EA, Nelsen CJ, Melissa M, Mullany JE, et al. NIH Public Access. 2014;7(14):2215–24.
71. Harbour JW, Dean DC. The Rb / E2F pathway: expanding roles and emerging paradigms. 2000; (314):2393–409.

72. Marescal O, Cheeseman IM. Cellular Mechanisms and Regulation of Quiescence. Dev Cell. 2020 Nov;55(3):259–71.
73. Rodda DJ, Chew JL, Lim LH, Loh YH, Wang B, Ng HH, et al. Transcriptional regulation of Nanog by OCT4 and SOX2. J Biol Chem. 2005;280(26):24731–7.
74. Yu Z, Pestell TG, Lisanti MP, Pestell R. Cancer Stem Cells. Int J Biochem Cell Biol. 2012;44(12):2144–51.
75. Kitano H. Biological robustness. Nat Rev Genet. 2004;5:826–37.
76. Álvarez-Buylla ER, Chaos Á, Aldana M, Benítez M, Cortes-Poza Y, Espinosa-Soto C et al. Floral morphogenesis: Stochastic explorations of a gene network epigenetic landscape. PLoS ONE. 2008.
77. Santangelo L, Marchetti A, Cicchini C, Conigliaro A, Conti B, Mancone C et al. Stable Repress Mesenchymal Program Is. 2012;2063–74.
78. Yang M, Li S, Anjum KM, Gui L, Zhu S, Liu J et al. A double-negative feedback loop between Wnt – b -catenin signaling and HNF4 a regulates epithelial – mesenchymal transition in hepatocellular carcinoma. 2013;5692–703.
79. Yang M, Chen C, Chau G, Chiou S, Su C, Chou T et al. Comprehensive Analysis of the Independent Effect of Twist and Snail in Promoting Metastasis of Hepatocellular Carcinoma. 2009;1–3.
80. Yin L, Ghebranious N, Chakraborty S, Sheehan CE, Ilic Z, Sell S. Control of mouse hepatocyte proliferation and ploidy by p53 and p53ser246 mutation in vivo. Hepatology. 1998;27(1):73–80.
81. Itahana K, Dimri G, Campisi J. Regulation of cellular senescence by p53. 2001;2791:2784–91.
82. Huschtscha LI, Reddel RR. p16 INK4a and the control of cellular proliferative life span. 1999;20(6):921–6.
83. Sheahan S, Bellamy COC, Treanor L, Harrison DJ, Prost S. Additive effect of p53, p21 and Rb deletion in triple knockout primary hepatocytes. Oncogene. 2004;23(8):1489–97.
84. Brown JP, Wei W, Sedivy JM. Bypass of senescenoe after disruption of p21(CIP1)/(WAF1) gene in normal diploid human fibroblasts. Sci (80-). 1997;277(5327):831–4.
85. Mayhew CN, Bosco EE, Fox SR, Okaya T, Tarapore P, Schwemberger SJ, et al. Liver-specific pRB loss results in ectopic cell cycle entry and aberrant ploidy. Cancer Res. 2005;65(11):4568–77.
86. Chicas A, Wang X, Zhang C, Mccurrach M, Zhao Z, Mert O, et al. Article Dissecting the Unique Role of the Retinoblastoma Tumor Suppressor during Cellular Senescence. Cancer Cell. 2010;17(4):376–87.
87. Miura S, Suzuki A. Induction of Steatohepatitis and Liver Tumorigenesis by Enforced Snail Expression in Hepatocytes. 2020;190(6).
88. Zhou D, Conrad C, Xia F, Park JS, Payer B, Yin Y, et al. Mst1 and Mst2 Maintain Hepatocyte Quiescence and Suppress Hepatocellular Carcinoma Development through Inactivation of the Yap1 Oncogene. Cancer Cell. 2009;16(5):425–38.
89. Shang X, Zhu H, Lin K, Tu Z, Chen J, Nelson DR et al. Stabilized b -catenin promotes hepatocyte proliferation and inhibits TNF a -induced apoptosis. 2004;332–41.

90. Xue W, Zender L, Miething C, Dickins RA, Hernando E, Krizhanovsky V et al. Senescence and tumour clearance is triggered by p53 restoration in murine liver carcinomas. 2007;445(February).
91. Al-Khalaf HH, Aboussekhra A. p16INK4A induces senescence and inhibits EMT through microRNA-141/microRNA-146b-5p-dependent repression of AUF1. Mol Carcinog. 2017;56(3):985–99.
92. Ma YC, Yang JY, Yan LN. Relevant markers of cancer stem cells indicate a poor prognosis in hepatocellular carcinoma patients: A meta-analysis. Eur J Gastroenterol Hepatol. 2013;25:1007–16.
93. Mohan A, Raj Rajan R, Mohan G, Kollenchery Puthenveettil P, Maliekal TT. Markers and Reporters to Reveal the Hierarchy in Heterogeneous Cancer Stem Cells. Vol. 9, Frontiers in Cell and Developmental Biology. 2021. p. 1–19.
94. Dhar D, Antonucci L, Nakagawa H, Kim JY, Glitzner E, Caruso S, et al. Liver Cancer Initiation Requires p53 Inhibition by CD44-Enhanced Growth Factor Signaling. Cancer Cell. 2018;33(6):1061–77.
95. Schwab JD, Kühlwein SD, Ikonomi N, Kühl M, Kestler HA. Concepts in Boolean network modeling: What do they all mean? Computational and Structural Biotechnology Journal. 2020.
96. Müssel C, Hopfensitz M, Kestler HA. BoolNet — an R package for generation. reconstruction and analysis of Boolean networks. 2010;26(10):1378–80.

Figures

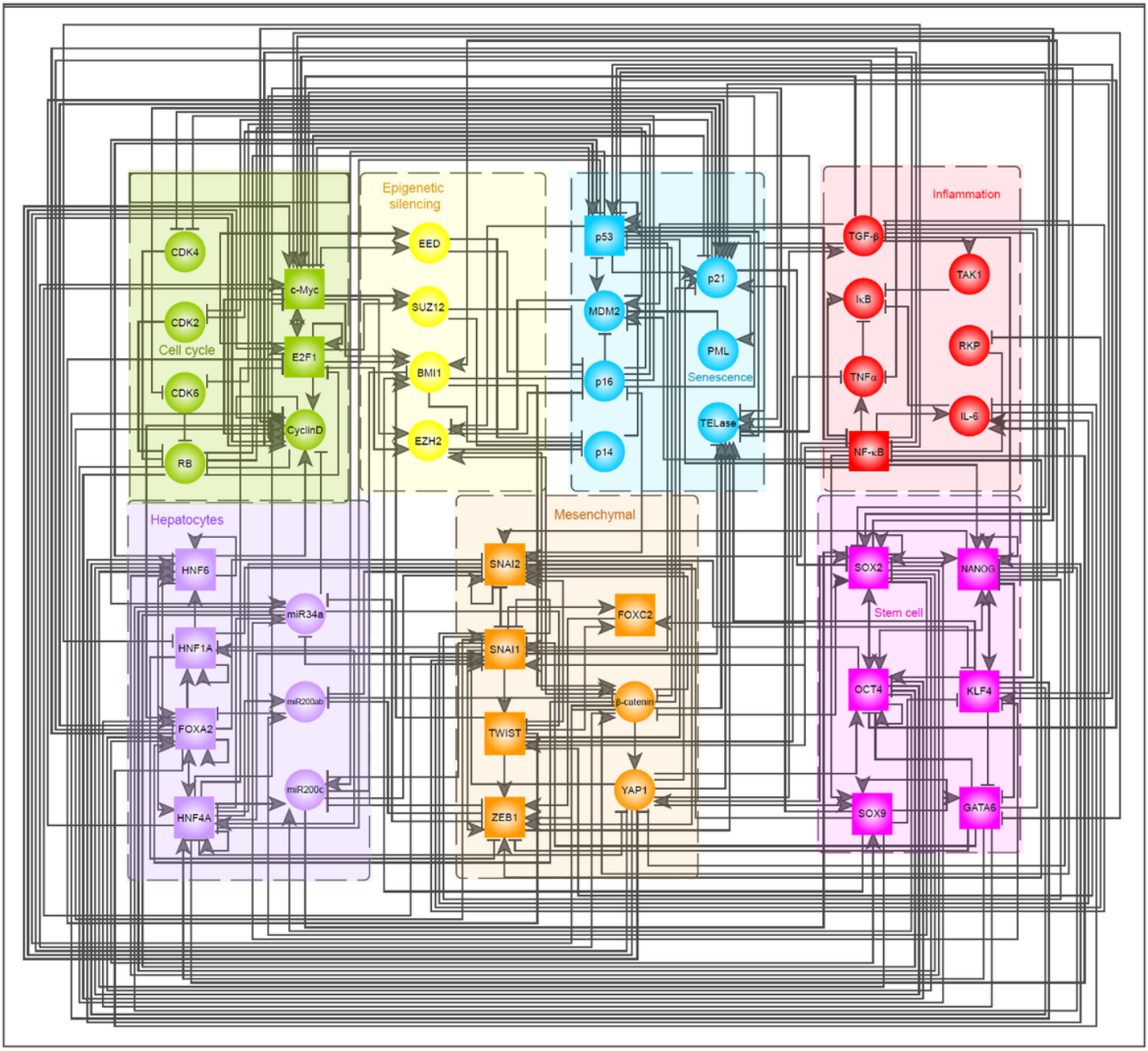

Figure 1

Full gene regulatory network of hEMT. In this figure we show the complete hEMT network. The square-shaped nodes are TFs, and the circular nodes are other biological molecules. Interactions ending in T-bar are inhibitions and those ending in an arrow are activations. In this figure, violet, orange and pink are exclusive markers of hepatocytes, mesenchymal cells and stem cells, respectively. On the other hand, green, blue, yellow and red are used to represent nodes of intracellular processes such as cell cycle, senescence, epigenetic silencing and inflammation. See additional file 1 (Additional File 1) to obtain more details about all biological interactions described here.

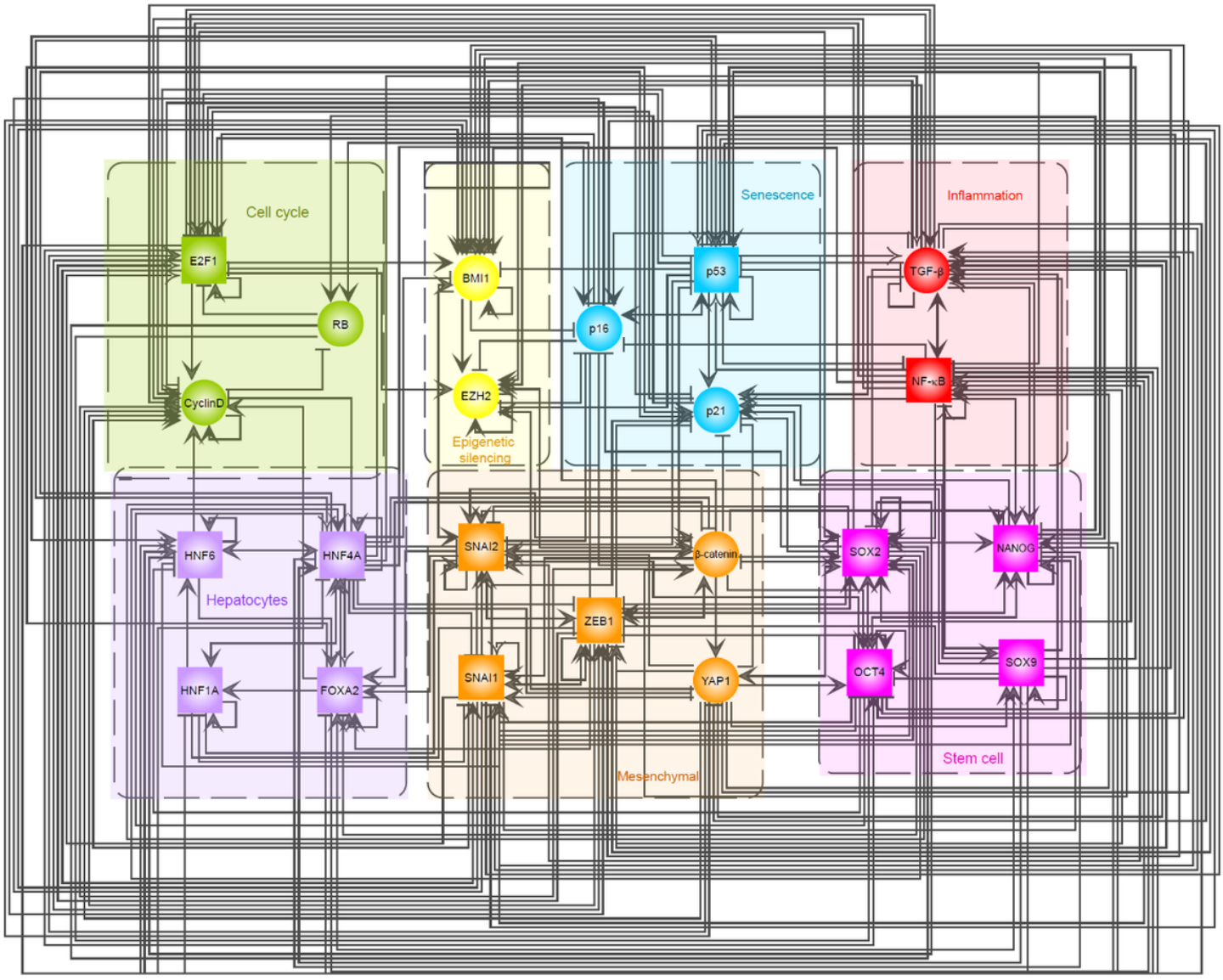

Figure 2

Reduced network of hEMT. In this figure we show the reduced hEMT GRN. As well as in the last figure, square-shape nodes are TFs, circular nodes are other biological molecules, interactions ending in T-bars are inhibitions, interactions ending in arrows are activations and dual interactions are ending in V-inverted shape. See additional file 3 (Additional File 3) to obtain more details about the reduction outcomes.

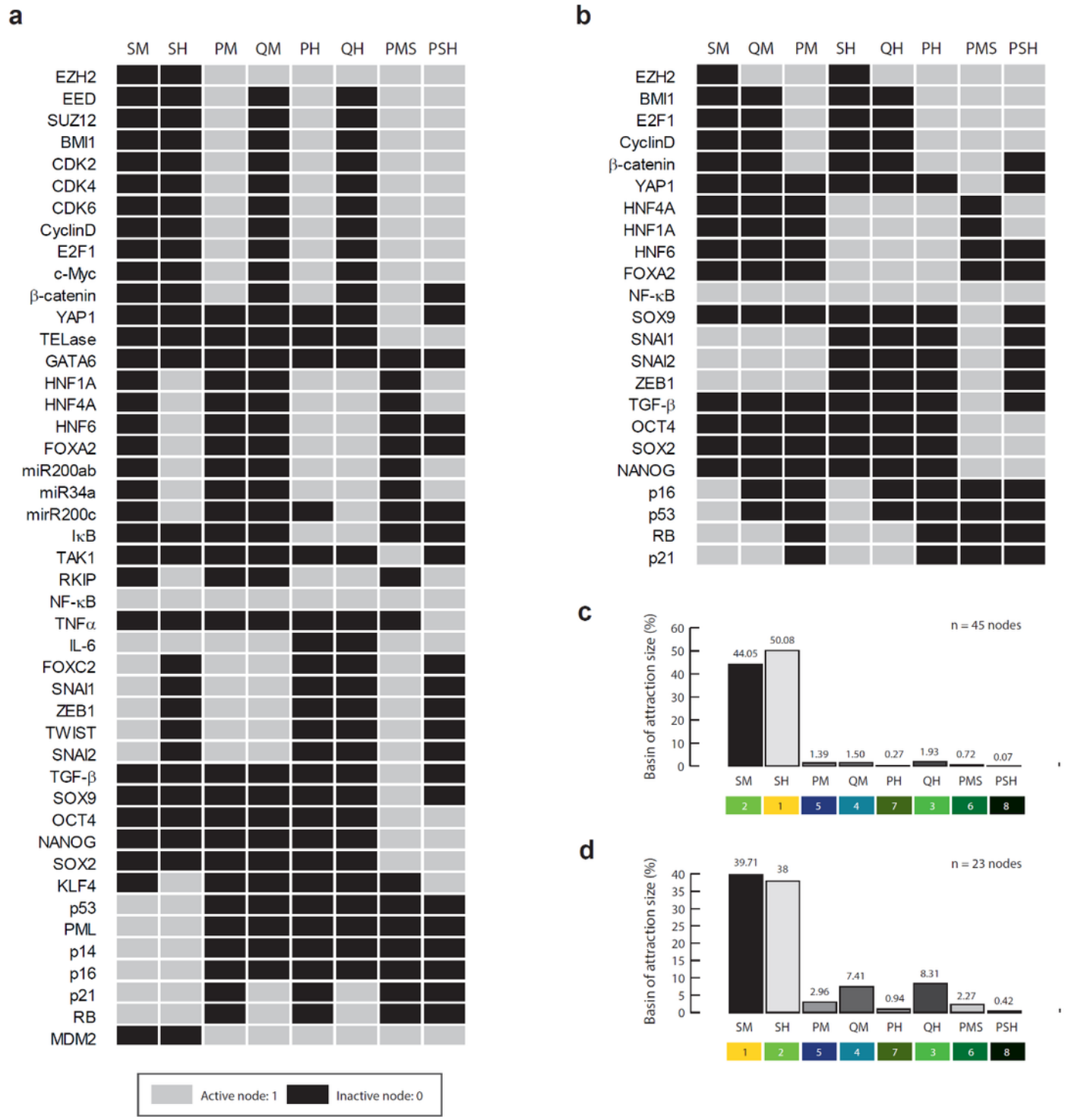

Figure 3

Phenotypic diversity of hEMT. Both models show that hEMT model produces senescent hepatocytes (SH), senescent mesenchymal cells (SM), quiescent hepatocytes (QH), quiescent mesenchymal cells (QM), proliferative hepatocytes (PH), proliferative mesenchymal cells (PM), proliferative stem-like hepatocytes (PSH), and proliferative stem-like mesenchymal cells (PMS). (a) Extended model provides more details about genetic profile of each phenotype, while (b) reduced model maintains the simplified

essence of each phenotype. The frequencies of each phenotypic attractor are given by the size of their basins of attraction, and both, extended model (c) and reduced model (d) present similar characteristics at qualitative level. Thus, we concluded that reduction maintains enough information of the extended model.

a

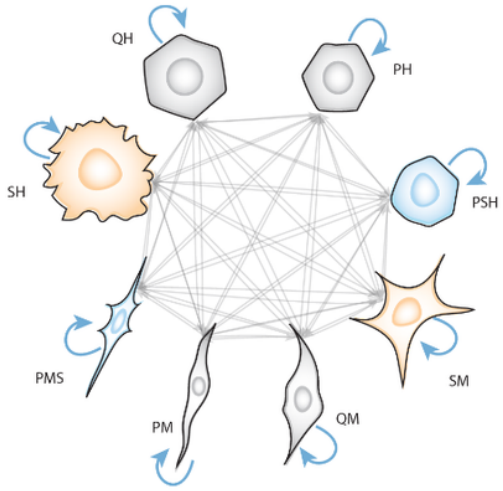

b

	SM	QM	PM	SH	QH	PH	PMS	PSH
SM	0.985999	0.004209	0.000448	0.008695	0.000415	0.000015	0.000219	0.000000
QM	0.024577	0.944689	0.013881	0.001596	0.012180	0.000142	0.002920	0.000014
PM	0.020804	0.037075	0.922308	0.000592	0.002368	0.005052	0.011756	0.000044
SH	0.013377	0.000170	0.000016	0.982650	0.003610	0.000109	0.000027	0.000040
QH	0.002400	0.011182	0.001388	0.028032	0.947790	0.006480	0.000679	0.002048
PH	0.003043	0.000662	0.015093	0.020966	0.037192	0.916706	0.003070	0.003269
PMS	0.013517	0.014534	0.025171	0.002344	0.003300	0.002015	0.935857	0.003261
PSH	0.000259	0.000312	0.000324	0.021323	0.045071	0.012166	0.020390	0.900155

Figure 4

Evaluation of physiological feasibility of hEMT network. Reduced model of hEMT proved to be stable against physiological stochastic noise. (a) Diagram that illustrates the procedure that was used to test the robustness of the GRN. In this stochastic process, we calculate the probabilities that one phenotype transitions to another in an indeterminate instant of time (represented with arrows). The probability that a phenotype will be maintained over time (blue arrows) is a measure of the robustness and stability of the phenotype in the face of normal physiological changes. (b) This matrix of Markov shows all probabilities represented in the last panel, where blue cells are the probabilities to conserve each phenotype over the time. These results show that the GRN of hEMT is robust against stochastic perturbations, which indicates that hEMT phenotypes are physiologically feasible.

Figure 5

Visualizing the effect of mutations on hEMT attractor landscape. This figure shows the outcomes of exploring the effect of different reported mutations on hEMT behavior. (a) Graphical representation of the basin of attraction size under different mutations. Here is shown that mutations like KO HNF4A abrogate hepatocyte phenotype, contributing to increase mesenchymal phenotypes. (b) Heat map showing the net effect of mutations on hEMT. The blue color indicates the decreases that an attraction basin presents with respect to the WT value. The red color shows the gain with respect to the reference value of the wild type. This heatmap shows that knockouts in HNF4A and HNF1A enhances mesenchymal phenotypes, as well as overexpression of SNAI1 and SNAI2. On the other hand, knockouts in p53 and p16 downregulate senescent phenotypes and increase quiescent and proliferative phenotypes. Therefore, these results reveal non-trivial details about functional changes on hEMT produced by mutations.

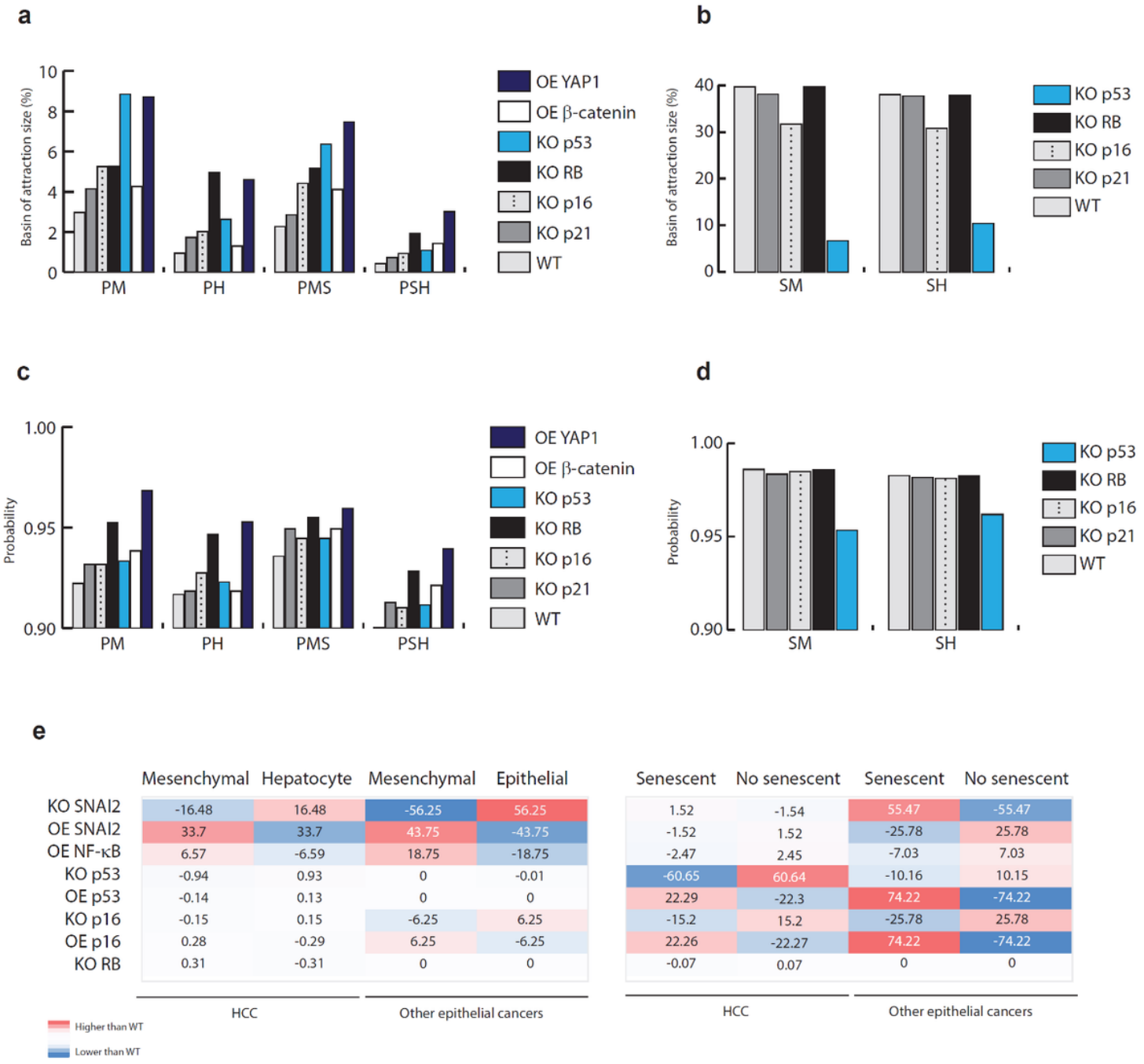

Figure 6

Somatic mutations increase CSCs in HCC. This figure shows the effect of somatic mutations on tumor suppressors like p53, p16, RB and p21, as well as aberrant activation on oncogenes such as b-catenin and YAP1. (a) Changes in the size of the basins of attraction of the proliferative phenotypes due to the action of the mutations. (b) Changes in the size of the attraction basins of the senescent phenotypes. (c) Changes in the robustness of the proliferative phenotypes due to the action of somatic mutations. (d) Changes in robustness due to the action of somatic mutations in senescent phenotypes. (e) Comparison of the effect of somatic mutations on HCC vs. other cancers.

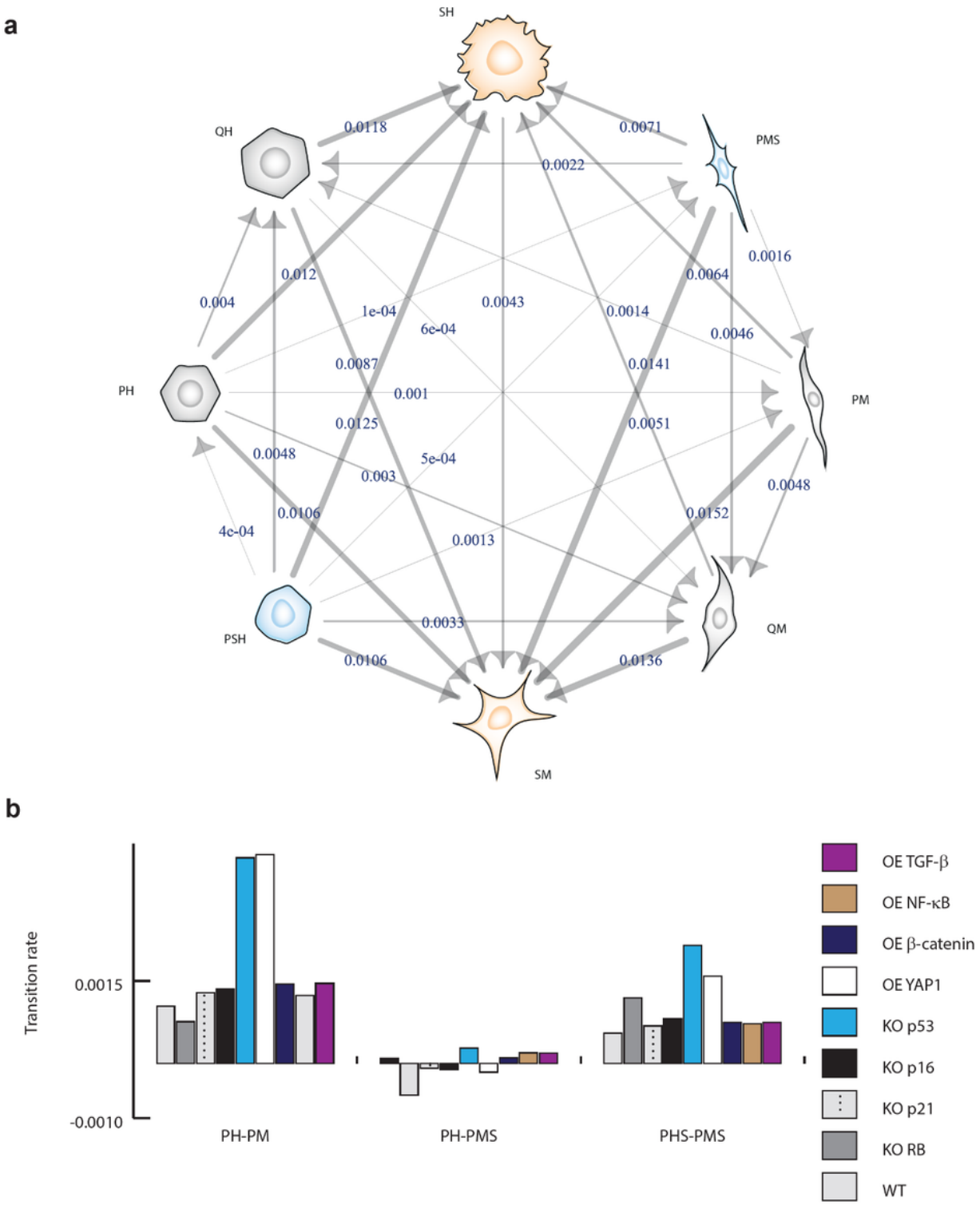

Figure 7

Differentiation pathways of hEMT. This figure shows the different pathways and cell fates that a hepatocyte can acquire when hEMT is activated. (a) Map of the different differentiation pathways that the phenotypes can follow. The numbers in blue correspond to the transition indices calculated for the wild type hepatocyte, the thickness of the arrows is proportional to the numerical value of the index. (b) Visualization of the effect of somatic mutations on differentiation pathways in hEMT. In particular, this

figure shows the effect of inhibiting tumor suppressors such as p53, p21, p16 and RB, as well as overexpressing oncogenes such as YAP1 and b-catenin, along with immune response genes such as NF-kB and TGF-b.

Supplementary Files

This is a list of supplementary files associated with this preprint. Click to download.

- AdditionalFile1HernandezMaganaetal2023.pdf
- AdditionalFile2HernandezMaganaetal2023.pdf
- AdditionalFile3HernandezMaganaetal2023.pdf
- AdditionalFile4FigHernandezMaganaetal2023.pdf